Journal Name

Journal of Materials Chemistry B

ARTICLE TYPE

Nanoparticle phosphate-based composites as vehicles for antimony delivery to macrophages: possible use in leishmaniasis

Betânia Mara Alvarenga,[a] **Maria Norma Melo,**[b] **Fréderic Frézard,**[c] **Cynthia Peres Demicheli,**[d] **Juliana Moreira Mendonça Gomes,**[a] **José Bento Borba,**[d] **Nivaldo Lucio Speziali**[e] **and José Dias Corrêa Junior***[a]

Pentavalent antimonial drugs such as *N*-methylglucamine antimonate (Glucantime®) are used for treating leishmaniasis but produce severe side effects, including cardiotoxicity and hepatotoxicity. We characterized the physicochemical properties of 3 nanoparticle phosphate-based composites (NPCs; NPC0, NPC3, and NPC5) as Sb(V) carriers for specifically targeting macrophages and reducing systemic side effects. NPCs were synthesized in liquid media and sterilized at 25 kGy before use. Macrophage viability and NPC toxicity, independent of Sb uptake, were evaluated to assess NPC safety in visceral leishmaniasis treatment. NPC zeta potential, conductivity, diameter, Sb content, and crystallinity were determined using electrophoretic light scattering, scanning electron microscopy (SEM), conductance, graphite furnace atomic absorption spectrometry (GFAAS), and X-ray diffraction, respectively. *In vitro* NPC cytotoxicity against murine peritoneal macrophages was evaluated using MTT assays, and Sb amounts internalized by macrophages were determined using GFAAS. The rate of macrophage infection with *Leishmania infantum* was assayed *in vitro*, with Glucantime® used as a reference drug. NPCs featured negative zeta potentials (-15.5 to -19.5 mV), mean diameters around 180 nm, and a low dissolution constant in Milli-Q water (<0.0197 mS cm^{-1}), and were prepared using 0.0 (NPC0) to 36.2 µg mL^{-1} Sb (NPC5). NPC5 exhibited characteristic crystalline peaks resembling mopungite, but other NPCs exhibited predominantly amorphous structures. Cell viability was not markedly affected at any NPC concentration tested. Light microscopy, SEM, and GFAAS data revealed NPC internalization and intracellular Sb retention. Amastigote infection was reduced by both Sb-containing NPC3 and Sb-lacking NPC0, but NPC3 was more effective. These data indicate the potential of NPCs as Sb nanocarriers for specifically targeting macrophages and lowering Sb dosage without reducing leishmanicidal activity.

Introduction

Leishmaniasis, a disease caused by an intracellular parasite, is endemic in 98 countries on 5 continents. Leishmaniasis occurs in 4 forms: cutaneous, diffuse cutaneous, mucocutaneous, and visceral. Visceral leishmaniasis is one of the most severe forms of the disease, being lethal in most untreated cases, and is caused by *Leishmania infantum* or *Leishmania donovani*. The disease is characterized by irregular fever, weight loss, hepatomegaly, splenomegaly, lymphadenopathy, and anemia. In America, the main sand fly species involved in transmission is *Lutzomyia longipalpis*. Dogs, which represent the most important domestic reservoirs of the disease, are responsible for the maintenance of parasitism in endemic foci due to the presence of amastigotes in the skin.[1,2]

The conventional treatment used for all forms of leishmaniasis relies primarily on intramuscular or intravenous administration of metal salts in the pentavalent form. *N*-methylglucamine antimonate (Glucantime®) is a drug of first choice due to its therapeutic efficacy.[3-7] The reduction of Sb(V) to Sb(III) is required for leishmanicidal activity, suggesting that Sb(V) is a pro-drug that becomes active and toxic after its reduction to Sb(III) in the body, which occurs inside phagolysosomes in macrophages.[5-7]

Although drugs containing Sb(V) remain the drug of choice in most cases of leishmaniasis, their hepatotoxicity, cardiotoxicity, and nephrotoxicity present serious obstacles to properly treating disease cases, and this can lead to treatment failure, interruption, or even discontinuation by the patient prior to the termination of chemotherapy.[8-11] Moreover, the medical care costs associated with the side effects of these chemotherapies are substantial and increase the overall economic burden. Therefore, current chemotherapies of leishmaniasis present several limitations.[12]

Nanostructured materials possess unique properties and capabilities that make them suitable for interaction with biological targets, particularly in drug-delivery applications.[13,14] As a drug-delivery vehicle, inorganic nanoparticles have received considerable attention due to their high cellular uptake, low toxicity, and low immune response; these nanoparticles are typically more hydrophilic, biocompatible, and stable as compared to organic materials.[15-21] Because of their several favorable characteristics, certain types of phosphate-based nanoparticles have been used in applications such as the delivery of DNA plasmids (pEGFP-N1, pUC19, *pSVβgal*) into the HeLa cell line[22] and delivery of antibiotics such as vancomycin to

prevent infections after knee arthroplasty,[23] and for use as a carrier in the oral administration and intestinal absorption of insulin in diabetic rats.[21] These diverse examples of applications reveal the potential for new therapeutic approaches.

5   In this study, we sought to synthesize nanoparticle phosphate-based composites (NPCs) containing Sb(V) and characterize their physicochemical properties, with a focus on their potential use in leishmaniasis therapy.

Experimental

Synthesis of nanoparticle phosphate-based composites

The complete synthesis of NPCs is presented in the patent filings BR 102012032493-8 and BR 102013032731-0, which are
15 available at www.inpi.gov.br. NPCs were synthesized using a mixture of salt solutions in a controlled precipitation system. The NPCs were prepared in solutions consisting of 7–10 mmol of $Na_4P_2O_7 \cdot 10H_2O$ (Cromoline), 5 mmol of $CaCl_2 \cdot 2H_2O$ (Cromoline), 5 mmol of $MgCl_2 \cdot 6H_2O$ (Synth), and 0–5 mmol of
20 $KSb(OH)_6$ (Sigma) by using semipermeable membranes (Spectrum Medical Industries, Inc.). We prepared 3 types of NPCs: NPC0 (no Sb added in the formulation), NPC3 (1.5 mmol of Sb salt added), and NPC5 (2.5 mmol of Sb salt). After synthesis, each NPC suspension was centrifuged at 3,500 rpm for
25 10 min, and the precipitate was washed thrice with absolute ethanol (Merck) and dried at 60 °C for 48 h. Lastly, aliquots of 0.1 g per vial of each NPC were placed in conical polypropylene microtubes and sterilized with 25 kGy gamma irradiation, at the Laboratório de Irradiação Gama - LIG, CDTN-UFMG. For all
30 subsequent analyses, a stock solution containing 1 mg of NPCs was eluted in 100 μL of liquid (Milli-Q water, ethanol, or RPMI 1640 culture medium) immediately before use.

Characterization techniques

35 Zeta potential and conductivity were measured (in mV and mS cm^{-1}, respectively) using a zetasizer (Nano ZS90, Malvern Instruments, UK); 20 μL of the NPC stock solution (1 mg diluted in 100 μL of Milli-Q water) was added to 2 mL of Milli-Q water in a folded capillary cell. For electron microscopy analysis, one
40 drop of the eluted stock solution of NPC (1 mg diluted in 100 μL of ethanol) was placed on carbon coverslips (Thermanox®) and dried. Samples were mounted on a stub with adhesive double-layered carbon tape and carbon sputtered at 10^{-5} mBar by using a Hitachi HUS4G. Electron micrographs (in the 50,000×
45 magnification range) were obtained with secondary electrons by using an FEG Quanta 200 (FEI). The NPC diameter distribution was determined using Image Pro Plus 4.0 and GraphPad Prism 5.0. The Sb content in NPCs was determined using graphite furnace atomic absorption spectroscopy (GFAAS).[28] Aliquots of
50 0.1 g of each NPC (NPC0, NPC3, and NPC5) were diluted in 1 mL of 0.2% HNO_3 solution for measuring Sb by using a spectrometer equipped with a graphite furnace and an autosampler (AAnalyst 600, Perkin Elmer). For determining the NPC crystallinity, we deposited 3 mg of each NPC on a silicon
55 sample port and analyzed them by means of X-ray diffraction (XRD) on a Geigerflex-RIGAKU diffractometer featuring a Cu pump, with a *2θ* scan angle and pitch of 0.1°, in an accumulation period of 1 h at room temperature. Data were collected using OriginPro 8 Sr0 v.80724 (B724) software. For all NPCs, XRD
60 patterns containing the intensity distribution of the beam

diffracted by the distinct crystal planes or amorphous patterns were obtained. To identify known crystal planes that were comparable to those obtained experimentally, the XRD patterns were compared with standard crystallographic data deposited in
65 these electronic databases: Inorganic Crystal Structure Database http://icsd.fizkarlsruhe.de.fisica.dotlib.com.br/search/basic.xhtml and CRYSTMET http://bdec.dotlib.com.br/go_global/index?direct=true&embed=false&app=crystmet

70

Biological assays

A commercial sample of meglumine antimoniate (Glucantime®) (5-mL vials at 300 mg mL^{-1}; Batch 3680, Sanofi-Aventis, São Paulo, Brazil) was obtained from the Brazilian Ministry of
75 Health. BALB/c mice (female, 4–6 weeks old, 18–22 g) were obtained from Cebio, Universidade Federal de Minas Gerais (UFMG, Belo Horizonte, MG, Brazil). Mice were provided *ad libitum* access to a standard diet and tap water. *L. infantum* promastigotes of the MHOM/BR/70/BH46 strain were cultured
80 *in vitro* at 24 ± 1 °C in RPMI 1640 medium supplemented with 10% fetal bovine serum and maintained through serial subculturing performed every 48–72 h. To isolate peritoneal macrophages, BALB/c mice were inoculated intraperitoneally with 2.5 mL of thioglycolate at 3% [24] After 3 days, animals were
85 sacrificed through cervical dislocation and 10 mL of cold, sterile unsupplemented RPMI medium was injected into the peritoneal cavity; the abdomen was then massaged to optimize the withdrawal of RPMI medium containing macrophages by using a syringe. The collected cells were centrifuged at 3,000 rpm for 15
90 min and then counted in a Neubauer chamber. This protocol was approved by the Ethics Committee for Animal Experimentation of the UFMG (CETEA protocol number 131/2012).

Murine macrophage cytotoxicity assay

95 To assess *in vitro* cellular toxicity, NPCs containing or lacking Sb were incubated in RPMI 1640 medium together with 5×10^5 murine macrophages in a 96-well microplate.[25] For each NPC, a stock solution (1 mg of NPC diluted in a final volume of 100 μL) was prepared and diluted to various concentrations (1, 0.1, 0.01,
100 0.001, and 0.0001 mg mL^{-1}) with RPMI 1640 complete medium. The Sb content ranged from 0.362 to 0.000 μg per well. As a negative control, adherent macrophages were incubated in the presence of only RPMI 1640 complete medium. Triplicate cultures were incubated for 24 h at 37 °C under a 5% CO_2
105 atmosphere. After incubation, 10 μL of a 5 mg mL^{-1} MTT (3-(4,5-dimethylthiazol-2-yl)-2, 5-diphenyltetrazolium bromide) solution (Sigma) was added to the wells (50 μg/well), and the cells (in 96 wells) were maintained for 4 h at 37 °C in a 5% CO_2 atmosphere. The supernatants were then removed and 100 μL of
110 dimethyl sulfoxide was added to dissolve the formazan crystals generated in the wells. The plates were subsequently read using a spectrophotometer, at a wavelength of 570 nm.[26-28] To obtain the final optical density (OD) values, the OD of the wells containing only macrophages (negative control) was subtracted from the
115 measured OD values.

Table 1: Zeta potential and conductivity of NPCs.

NPC	Zeta potential (mV)	Conductivity (mS cm^{-1})
NPC0	-19.5	0.00842
NPC3	-17.8	0.0136
NPC5	-15.5	0.0197

Measurement of intracellular Sb in murine macrophages

The internalization of Sb into macrophages was examined using
5 GFAAS.[29] Macrophages (5×10^5) in a final volume of 1 mL were
maintained in 24-well plates at 37 ºC in a 5% CO_2 atmosphere.
The macrophages were allowed to adhere for 2 h and then 6 μL
of NPC3 and NPC5 stock solutions (0.1 g diluted in a final
volume of 100 μL) were added for either 24 or 48 h. After the
10 incubation, cells were washed thrice with RPMI 1640 medium to
remove all free NPCs and Sb. Cells were allowed to recover and
then digested in 65% HNO_3 (Merck) overnight, which was then
diluted 100-fold in 0.2% HNO_3 for subsequent measurement of
Sb by means of atomic absorption spectroscopy performed using
15 a spectrometer equipped with a graphite furnace and an
autosampler (AAnalyst 600, Perkin Elmer). The rates of Sb
internalization (R) at 24 and 48 h were calculated using this
formula: R = Sb (measured in 5×10^5 macrophages) / Sb
(measured in the NPCs added per well).

20

Effect of NPC0, NPC3, and Glucantime on *L. infantum* infection

Twenty-four-well plates containing peritoneal macrophages ($5 \times$
25 10^5) adhered on glass coverslips were incubated overnight at 37
°C under 5% CO_2 in the presence of promastigote (1×10^7)
parasites during the stationary growth phase in order to allow
infection. Wells were washed twice with the same media at room
temperature to remove non-internalized parasites. The time at
30 which the wells were washed was considered "time zero" of
infection. Different volumes of stock solutions (1 mg diluted in a
final volume of 100 μL) of NPC0 (lacking Sb) or NPC3
(containing Sb) were added to cells at final concentrations of 20,
60, and 180 μg mL^{-1}, which corresponded to Sb(V)
35 concentrations of 13.9, 41.7, and 125.1 ng mL^{-1} for NPC3,
respectively. NPCs were incubated with cells for 24, 48, and 72 h
at 37 °C under 5% CO_2. Glucantime was tested at concentrations
of 50, 150, and 450 ng mL^{-1}, which corresponded to Sb(V)
concentrations of 33.25, 99.75, and 299.25 ng mL^{-1}, respectively.
40 The control infection rate for the assays was >90%. Drug and
NPC activities were evaluated from Panótico-stained slides by
counting at least 200 cells per treatment, and the rates of infected
cells were assessed by calculating the percentage (%) of infected
cells in all treatments.[30,31] Reductions in the percentage of
45 infection by *L. infantum* and parasite residence within peritoneal
macrophages were evaluated by counting the infected
macrophages and the internalized parasites, respectively, after
various incubation times. The number of internalized parasites
was binned and also plotted according to a categorized infection
50 rate—uninfected, 1–5, 6–10, or >10 amastigotes per
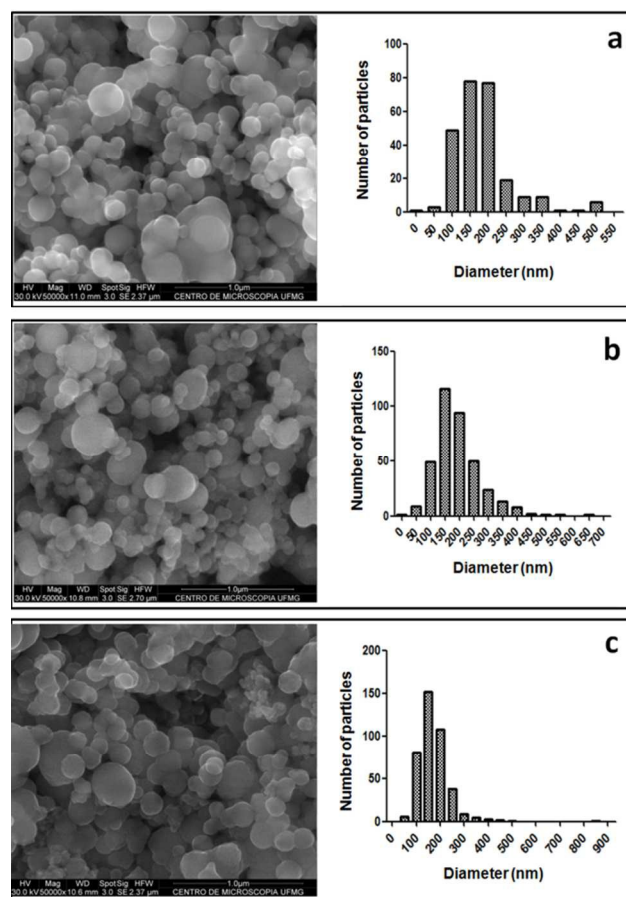macrophage—adapted from Gebre-Hiwot et al.[30,31]

55 **Fig. 1.** Scanning electron micrographs, obtained with secondary
electrons, of NPC0 (a), NPC3 (b), and NPC5 (c) and the
respective diameter distribution graphs.

60 **NPC internalization**

Leishmania-infected murine peritoneal macrophages were
obtained using procedures described in preceding paragraphs.
Macrophages were incubated with 20 μg mL^{-1} NPC0, NPC3, and
NPC5 for 24 h, and then Panótico-stained and imaged using an
65 Olympus BX 41 microscope equipped with an Olympus Q Color
3 digital camera and a 60× objective lens and a 2.5× projective
lens. Images were calibrated using a 0.01-mm micrometer ruler
(Olympus). For electron microscopy, *Leishmania*-infected
murine peritoneal macrophages were cultured using the
70 aforementioned procedures, and incubated with 60 μg mL^{-1}
NPC3 on carbon coverslips (Thermanox®). After incubation,
samples were fixed using 4% glutaraldehyde in cacodylate buffer
(0.1 M, pH 7.4) for 24 h. After post-fixation with 1% OsO_4, the
samples were rinsed with PBS and dehydrated using alcohol
75 solutions. Samples were then mounted on stubs and carbon
sputtered in an evaporator (Hitachi Model HUS4G) and analyzed
with secondary and back-scattered electrons by using a Quanta
FEG 3D FEI electron microscope**.**
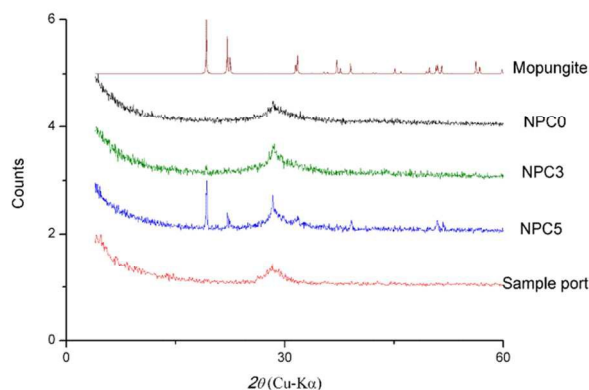
80

Fig. 2. XRD patterns of NPCs and mopungite. The amorphous pattern observed in the sample holder, NPC0, and NPC3 is distinct from the crystalline profile in mopungite and the mixed
5 profile in NPC5.

Results and discussion

10 The zeta potential and conductivity measured for each NPC are presented in Table 1. Negative zeta potentials were measured for the NPCs and ranged from -15.5 mV for NPC5 to -19.5 mV for NPC0. Conductivity values were close to 0.01 mS cm^{-1}.
Electron microscopy analysis revealed that the NPCs were
15 spherical (Fig. 1). The average diameter of NPCs and the diameter range of 95% of the nanoparticles were respectively the following: NPC0, 183.2 and 173.1–193.3 nm; NPC3, 193.5 and 185.2–201.8 nm; and NPC5, 172.8 and 166–179.6 nm. These data show a close diameter distribution among the synthesized
20 NPCs.
Antimony levels were higher in NPC5 nanoparticles (36.24 μg mL^{-1}) than in NPC3 nanoparticles (6.95 μg mL^{-1}). Sb levels in NPC0 particles, which were prepared without the addition of antimony, were below the limit of quantification (0.063 μg mL^{-1}
25). The XRD patterns of the NPCs (Fig. 2) revealed a single broad peak present at $2\theta = 28.3°$ for all synthesized nanoparticles, similar to the gate silicon samples, indicating a predominantly amorphous pattern. However, NPC5 also exhibited crystalline peaks (19.1 and 22.1), and this profile was similar to the
30 crystalline profile obtained for mopungite (NaSb(OH)$_6$).
The diameter distribution of a nanoparticle is one of its most critical features because it can determine the nanoparticle's distribution *in vivo*, biological fate, toxicity, targeting capacity, drug entrapment, release, and stability. A review article
35 previously noted that nanoparticles featuring a zeta potential near (+ -) 30 mV remain in suspension, where the charged surface is responsible for particles' dispersion and is favorable for *in vitro* and *in vivo* assays.[32] Studies on functionalized and non-functionalized calcium phosphate nanoparticles have reported
40 diameters and zeta potentials ranging from 40 to 200 nm and -11 to -28 mV,[21] respectively, which are similar to those in our study. These values are also similar to values reported for calcium phosphate nanoparticles containing porphyrin (250 nm and +1.2 and -18 mV[32] and 100–250 nm and +12 to -24 mV[33]). These data
45 suggest that NPCs can be consistently synthesized.
Nanoparticles featuring a diameter of 100–300 nm were shown to
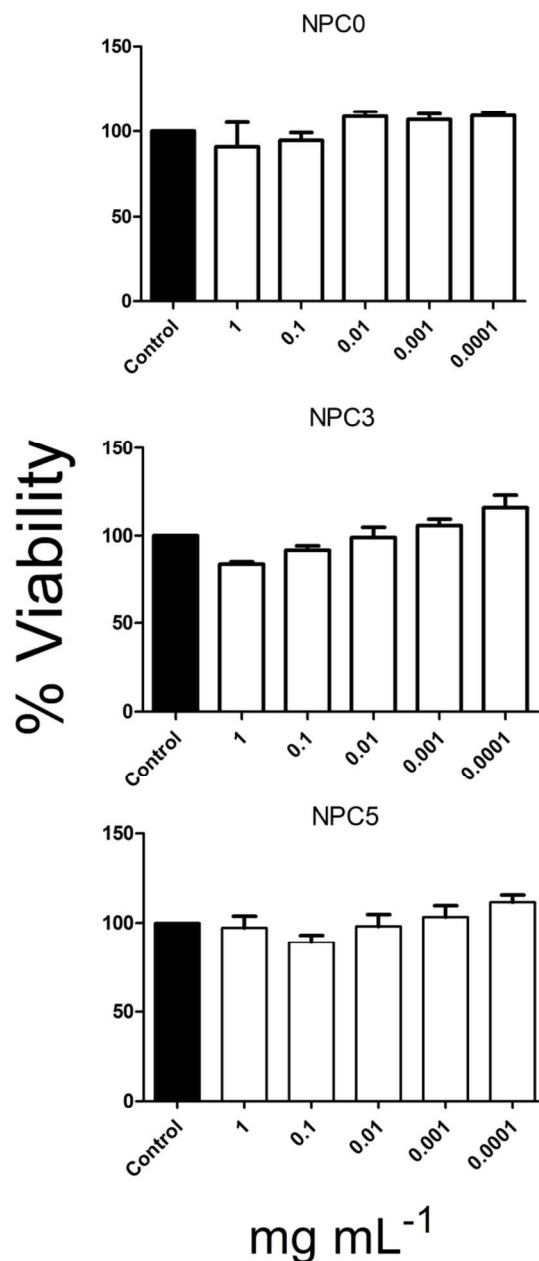

Fig. 3. Cell viability after incubation with NPC0, NPC3, and
50 NPC5. None of the nanoparticles exhibited significant toxicity toward murine macrophages (two-way ANOVA, p < 0.05).

be effective in cellular uptake studies, and the zeta potential of the nanoparticles varied according to their functionalization.[34]
55 Other studies have also reported that the uptake of nanoparticles by NIH3T3 fibroblasts occurred after only a few hours of exposure, and that porphyrin was released in the cytoplasm after dissolution of the nanoparticles, with no adverse effects being detected.[35]   Analysis   of   the   diameter   distribution
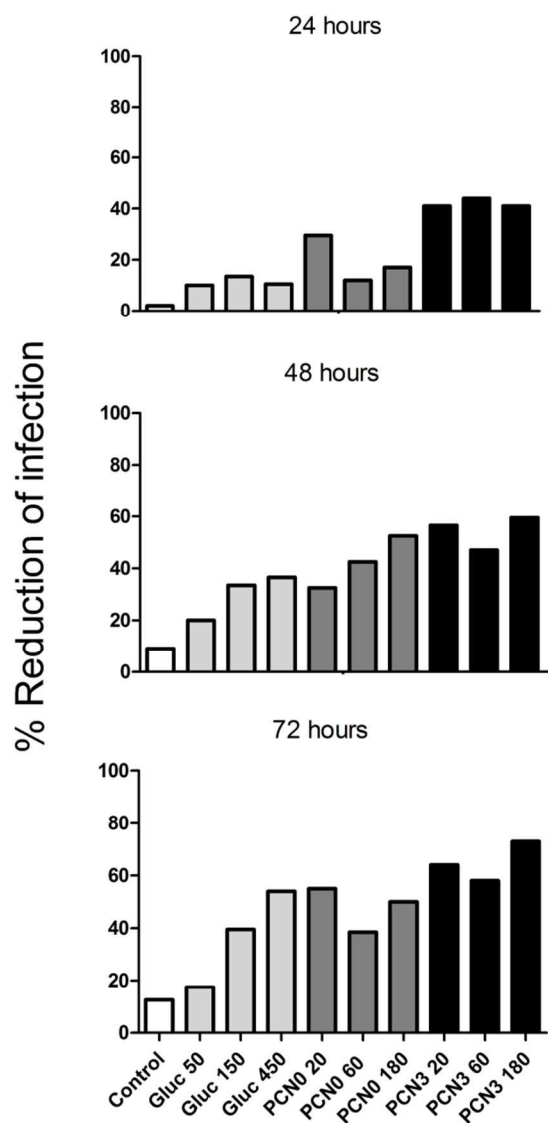
Fig. 4. Reduction of infection (%) at 24, 48, and 72 h after exposure to Glucantime (50, 150, and 450 ng mL^{-1}) and NPC0 and NPC3 (20, 60, and 180 µg mL^{-1}).

of NPC0, NPC3, and NPC5 indicated that 95% of the nanoparticles featured diameters of approximately 180 nm, and the data presented herein also suggest the dissolution of these nanoparticles. The conductivity values of NPCs near 0.01 mS cm^{-1} support their structural stability in liquid medium. The results showed a slight mobilization of the constituent elements of the NPCs. In XRD analysis, all NPCs showed an amorphous profile, except for NPC5. Amorphous minerals are highly soluble and can incorporate diverse organic and inorganic substances and mobilize their mineral ions.[36,37] To test the cytotoxic effect of NPCs on murine macrophages, the viability of the cells at distinct NPC concentrations was measured (Fig. 3). Cell viability was not affected in a statistically significant manner by any NPC at any concentration tested. Although the toxicity of nanoparticles could be lower than that of current chemotherapeutic agents, only a few studies have investigated inorganic nanoparticles as chemotherapeutic agents for leishmaniasis. Antimony sulfide

(Sb$_2$S$_5$) nanoparticles have been demonstrated to exhibit low toxicity toward uninfected macrophages and leishmanicidal activity against intracellular *L. infantum*.[38] Studies on selenium nanoparticles in macrophage cultures infected with *L. infantum* have demonstrated a reduction in the proliferation of promastigotes and amastigotes at 72 h, and an IC50 of 100 µg mL^{-1} in uninfected macrophages.[39] *In vitro* studies have been conducted on the anti-proliferative activity of 7 ternary Ni(II) complexes featuring a triazolopyrimidine derivative and different aliphatic or aromatic amines as auxiliary ligands against promastigote and amastigote forms of *L. infantum* and *Leishmania braziliensis*; the results showed that these complexes are not toxic to J774.2 macrophages[40,] despite the general toxicity of Ni.[41] Other studies investigated the activity of TiO$_2$@Ag nanoparticles (TiAg-NPs) against *L. infantum* and *L. tropica* in the presence of visible and non-visible light; these nanoparticles reduced the survival of *L. infantum* amastigotes inside macrophages in a concentration-dependent manner under both visible and non-visible light, although stronger effects were observed under visible light. Exposure to a low concentration (5 µg mL^{-1}) of TiAg-NPs under non-visible light showed no effect on amastigotes, similar to the control; however, at the same concentration but under visible light, TiAg-NPs inhibited amastigotes of *L. infantum* 3–5 times more effectively.[42]

Table 2 shows the quantification of Sb in macrophages exposed to NPC0, NPC3, and NPC5 for 24 or 48 h and the respective Sb content increase relative to the control. All macrophages exposed to NPCs containing Sb showed a high cellular uptake of Sb, the highest levels being obtained with NPC5. After treatment for 48 h with NPC0, cellular levels of Sb were below the quantification limit, similar to the Sb levels in controls. After 24 h, Sb levels in macrophages treated with NPC3 were lower than those in cells treated with NPC5. However, after 48 h, the cellular Sb levels did not differ significantly in macrophages treated with NPC3 and NPC5.

Macrophages incubated with NPC5 exhibited a 47% reduction in cellular Sb concentrations between 24 and 48 h; by contrast, Sb concentrations decreased by only 19% over this period in macrophages treated with NPC3.The uptake of Sb by macrophages was observed within the first 24 h of interaction and this was followed by a reduction in the cellular Sb level over time, and the results suggested distinct elimination rates for the NPCs tested. The concentration of Sb in macrophages ranged from 3,596 µg L^{-1} (NPC5, 24 h) to 750 µg L^{-1} (NPC3, 48 h). NPC5 promoted a higher uptake of Sb at 24 h than the other nanoparticles did likely because the input concentration of Sb was 5 times higher, although Sb was also lost from the macrophages more rapidly by 48 h. The intracellular Sb level over time was more stable with NPC3 than with NPC5: the values varied within 20% of the input Sb concentration. These data suggest that distinct NPCs affect the intracellular Sb content differently. In several previous studies, Sb(III) levels after Glucantime exposure have been measured using different techniques,[43-50] but few studies have measured Sb(III) and Sb(V) levels in macrophages. Previous studies have quantified Sb(III) and Sb(V) levels in promastigotes and amastigotes of *L. mexicana pifanoi* by using absorption spectroscopy with electrothermal atomization.[29] This assay was also used here to characterize Sb(III) and Sb(V) influx and efflux kinetics. Influx rates were determined at antimony concentrations that produced a 50% inhibition of growth (IC50). The influx rates of Sb(V) into amastigotes and promastigotes were 4.8 and 12 pg/million cells/h, respectively, at an Sb concentration of 200 µg mL^{-1}. The influx rate of Sb(III) into amastigotes was 41 pg/million cells/h at an Sb concentration of 20 µg mL^{-1}. The influx of Sb(III) into

promastigotes at an Sb concentration of 1 μg mL^{-1} was rapid and reached a plateau of 175 pg/million cells in 2 h. The efflux of Sb(III) and Sb(V) from amastigotes and promastigotes exhibited biphasic kinetics: The initial (α) half-lives of Sb(V) and Sb(III) efflux were <4 min and 1–2 h, respectively, and the apparent terminal (β) half-lives ranged from 7 to 14 h. The highest concentration of intracellular Sb previously reported, approximately 90 μg L^{-1}, was measured in Mono Mac 6 human macrophages exposed to Sb(V) in the form of sodium stibogluconate (Pentostam).[51] By comparison, we observed considerably higher intracellular Sb concentrations in our work.

In macrophages exposed to Sb-containing NPCs, Sb retention could potentially occur in a manner similar to that previously described in the case of polysaccharide and potassium antimony tartrate Sb(III) or sodium stibogluconate Sb(V) in *Leishmania*-infected WR120 macrophage J774 cultures. After only 4 h, macrophages accumulated large amounts of Sb, which was retained intracellularly for at least 3 days, demonstrating a potential role of the cells as an Sb reservoir.[52] These cells are also commonly used as a target for testing potential therapeutics against leishmaniasis because of the cells' role as amastigote cleaners.[53-54] Nanoparticle-mediated targeting of Sb to macrophages could decrease the systemic side effects and also increase the efficacy of the treatment, and this has been demonstrated using several Sb-containing nanoparticles. Antimony encapsulated in liposomes was nearly 700 times more active than the non-encapsulated metallodrug.[55] Moreover, sodium stibogluconate encapsulated in tuftsin-bearing liposomes was at least 200 times more effective against *L. donovani* infection in hamsters than the non-encapsulated drug, which was effective only after 28 days of treatment.[56]

Despite the aforementioned benefits, the use of liposomes presents drawbacks such as the capture of liposomal preparations primarily by the liver, the limited efficiency of Sb encapsulation in vesicles, and possible side effects due to specific lipid components.[57] Therefore, other formulations have been investigated as promising alternatives for use as novel therapeutics. These formulations include amphiphilic complexes of Sb(V) and NPCs, which were designed for treating visceral leishmaniasis which have advantages compared to Glucantime.[58]

The results of MTT assays demonstrated that NPCs do not affect the viability of murine macrophages; moreover, the remobilization of the constituent elements present on the NPC structure (Mg, P, Cl, Ca, and eventually Sb) did not demonstrably affect the metabolic activity of macrophages. These data confirm previous reports of calcium phosphate nanoparticles being compatible with the maintenance of cell viability.[21,34,36]

When Glucantime was used at the highest tested dose (450 ng mL^{-1}), which is close to the IC50 reported by Tempone et al.,[27]

the percentage of infected cells was decreased over the experimental period, from 10% at 24 h to nearly 60% after 72 h (Fig. 4). Similar results were obtained with NPC0 at a low concentration of 20 μg mL^{-1}. NPC3 also reduced the percentage of infected cells, which ranged from 40% at 24 h to nearly 80% after 72 h. These results suggest that the presence of Sb in NPC3 enhanced the leishmanicidal activity of the nanoparticles. Moreover, the effects of NPC treatment were stronger at earlier exposure times.

Few studies have compared the efficacy of nanocarriers carrying or not leishmanicidal substances in reducing infections over time. In addition to the increased efficacy of nanocarried drugs demonstrated previously, the lack of toxicity observed with NPC0 and NPC3 highlights the safety of these treatments.[39,40,59,60] Glucantime did not significantly affect amastigote infection rates after 24 h (Fig. 5). However, after 48 h, the percentages of cells containing 6–10 and >10 amastigotes were reduced at all concentrations and the percentage of uninfected macrophages increased in a dose-dependent manner, reaching 40% at the highest concentration tested (450 ng mL^{-1}). After 72 h, the percentage of cells containing 6–10 amastigotes was reduced and the percentage of uninfected macrophages was increased in a dose-dependent manner and reached 50% at the highest concentration tested (450 ng mL^{-1}). As shown in Fig. 5, NPC0 treatment for 24 h of macrophages infected with *L. infantum* reduced the percentage of macrophages containing >10 amastigotes and increased the percentage of uninfected macrophages. After 48 h, the percentage of macrophages containing 6–10 or >10 amastigotes was reduced, and the percentage of uninfected macrophages was increased to ~60%. Similar results were observed after 72 h. NPC3 treatment reduced the percentage of macrophages containing 6–10 and >10 amastigotes and increased the percentage of uninfected macrophages, which was ~40% at the lowest concentration (20 μg mL^{-1}) after 24 h (Fig. 5). After 48 h, the percentages of macrophages containing 1–5, 6–10, and >10 amastigotes were reduced and the percentage of uninfected macrophages was increased to ~55% at the lowest concentration (20 μg mL^{-1}). After 72 h, the percentage of macrophages containing 1–5, 6–10, and >10 amastigotes was reduced (at 60 and 180 μg mL^{-1}), and the percentage of uninfected macrophages was increased to ~70% at the highest concentration tested (180 μg mL^{-1}).
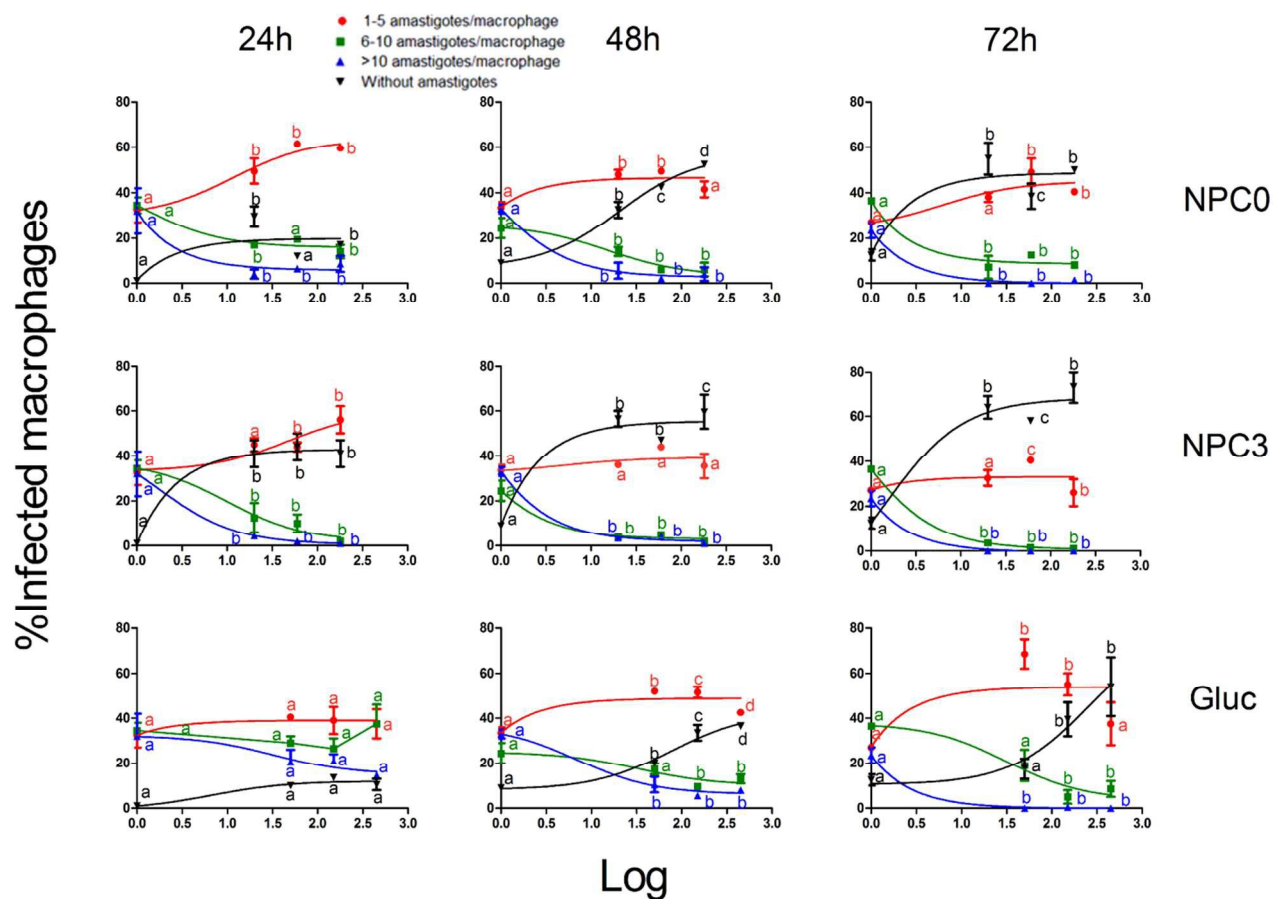
Fig. 5. Rates of macrophage infection by *L. infantum* amastigotes as a function of the concentrations of NPC0 and NPC3 (µg mL^{-1}) and Glucantime (ng mL^{-1}) after incubation for 24, 48, and 72 h. The labels a, b, c, and d indicate significant differences between points in the same category; two-way ANOVA with post-hoc Bonferroni test, $p < 0.05$.

5

10 **Table 2.** Antimony amounts (µg L^{-1}) added to cultures at time 0 h and obtained from 5×10^5 murine peritoneal macrophages after incubation with NPC0, NPC3, NPC5, and controls for 24 and 48 h. The total amounts of Sb added to cultures and the rates of Sb internalization into macrophages after incubation for 24 and 48 h are presented.

Treatment	0 h Sb added	24 h	48 h	Rate of Sb internalization, 24 h	Rate of Sb internalization, 48 h
Control	nd	33.5 [a]	30.7 [a]	nd	nd
NPC0	37.8 [a]	nd	28.7 [a]	nd	nd
NPC3	4,168 [c]	919.9 [b]	750.1 [b]	0.22	0.18
NPC5	21,745 [d]	3596.0 [c]	1912.0 [b]	0.16	0.09

15 "nd": not determined; superscripts a, b, c, and d: significant differences between points in the same category, two-way ANOVA with post-hoc Bonferroni test with – log (y) transformed data, $p < 0.05$. Mean values are presented.

NPC0 and NPC3, at all concentrations tested, exhibited leishmanicidal activity against *L. infantum* amastigotes at 24, 48, and 72 h. These results indicate that the effects of NPCs are not 20 associated only with the Sb content, despite a correlation between Sb levels and the treatments with Glucantime (Sb: 33.20, 99.75, and 299.25 ng mL^{-1}) and NPC3 (Sb: 14, 42, and 125 ng mL^{-1}). These data suggest that solubilized ions from NPCs can affect the cellular metabolism of both the host cell and 25 amastigotes. The effects at a low NPC3 concentration (20 µg mL^{-1}), were similar to those observed at 60 and 180 µg mL^{-1}, and dose-dependent effects were only observed after 24 h.
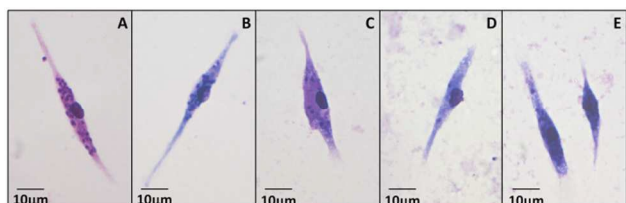
Fig. 6. Light microscopy images of macrophages infected with *L. infantum* after incubation for 24 h. Amastigotes appear as
basophilic dots in the cytoplasm of these Panótico-stained macrophages. Control (A), Glucantime at 50 ng mL^{-1} (B), and NPC0 (C), NPC3 (D), and NPC5 (E) at 60 μg mL^{-1}.

These data suggest that because of Sb retention, the low dose can produce a similar effect as the higher doses. By using light microscopy, we were able to identify infected murine macrophages that contained internalized *L. infantum* amastigotes. No morphological changes relative to control were observed in these cells as a result of Glucantime or NPC treatment (Fig. 6).

NPC3 internalization by macrophages was confirmed using SEM-associated techniques (Fig. 7 and S1-S5, ESI†). By using secondary electrons, we could clearly observe macrophage membrane covering the spherical nanostructures. Nanostructures were present at all time-points analyzed and preferentially localized to the distal portion of macrophages. Structures resembling spherical NPCs were rarely observed outside the macrophages, which reflected the active internalization of nanoparticles. Electron micrographs acquired using backscattered electrons confirmed the intracellular distribution of NPCs.

NPC0, whose composition did not include Sb, likely showed an effect against *L. infantum* due to the release of its ionic constituents inside macrophages. Phosphorous in the form of pyrophosphates, orthophosphates, or polyphosphates has been associated with cellular power generation mechanisms and could be related to the maintenance of cell viability, and no deleterious effects have been reported due to an increase in the intracellular concentration of these compounds.[61-67] Similarly, increasing the concentration of Sb(V) does not appear to affect macrophages, as observed in THP-1-lineage macrophages.[68] This behavior of Sb(V) differs from the behavior of both intracellular Sb(III) and Ca. Several of the side effects and the toxicity of Sb-based drugs are related to the concentration of Sb(III), which is highly toxic. The viability of THP-1 macrophages is reduced to 50% at an Sb(III) concentration of 20 μg mL^{-1}.[68] Currently, Sb(V) is hypothesized to act as a pro-drug, which is converted to Sb(III) inside acidic intracellular vacuoles (parasitophorous vacuoles in infected cells) such as macrophages. Sb(III) affects the enzymatic activity of the parasite, and this leads to trypanothione depletion and susceptibility to macrophage nitric oxide (NO) which is synthesized from arginine and O2 by NO synthase.. These events lead to parasite membrane disruption through peroxidation and the release of intracellular Ca stores, which frequently result in apoptosis.[7,69-74] We cannot rule out the possibility that the same mechanisms are induced after the internalization and dissolution of NPCs by macrophages, given that the introduction of Sb(V) into NPCs allows the delivery of Sb(V) into cells in which the parasite is internalized. Moreover, several macrophage mechanisms associated with parasite elimination depend on Ca^{+2} release from their own cellular stores. In phagocytosis, free
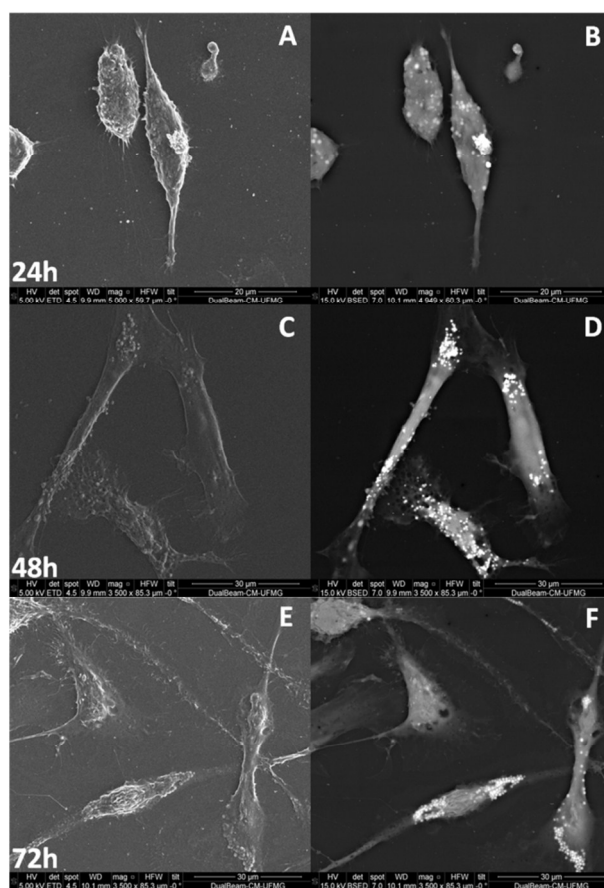

Fig. 7. Scanning electron micrographs of infected macrophages incubated with NPC3 (60 μg mL^{-1}); images were obtained after 24, 48, and 72 h of interaction. Typical secondary electron micrographs from the surface of macrophages are shown in A, C, and E. In electron micrographs acquired with backscattered electrons, NPCs appear as white dots inside macrophages (B, D, and F).

intracellular Ca^{+2} is required for the uptake of particles, phagosome maturation, cytoskeletal rearrangement, intravacuolar release of H$^+$, NADPH oxidase complex activation, and the generation of NO (oxidative burst).[75-80] These processes are initiated by the activation of phospholipase C and/or D by Fc receptors and/or complement receptors through store-operated calcium entry channels, which induce Ca^{+2} release.

Promastigotes can transiently prevent the fusion of phagosomes and lysosomes and thereby delay or inhibit endosomal maturation, as reflected by the late expression of Rab7 and LAMP-1.[81,82] Furthermore, lipophosphoglycan from *Leishmania* promastigotes inhibits endosome maturation by inducing periphagosomal F-actin accumulation[83] and prevents the acidification of phagosomes by interfering with the V-ATPase pump, and this allows promastigotes to differentiate into resistant amastigotes.[84] Conversely, NPC-induced Ca remobilization could block these processes and act as an adjuvant to the elevation of intracellular Ca^{+2}, and thus suppress Ca-dependent evasion mechanisms. The elevation of Ca inside vacuoles could potentially increase the apoptosis of parasites.

Conclusions

In this study we suggest that water-stable NPCs synthesized containing pyrophosphate, calcium, and magnesium and with or without antimony become soluble after macrophage uptake. The ionic constituents of the NPCs released inside the macrophages probably participate in the resolution of the parasitic processes examined here that occur within murine macrophages infected with *L. infantum.*

Notes

a Departamento de Morfologia, Instituto de Ciências Biológicas, Universidade Federal de Minas Gerais, Av. Antônio Carlos 6627, Pampulha, 31270-901 Belo Horizonte, MG, Brazil

b Departamento de Parasitologia, Instituto de Ciências Biológicas, Universidade Federal de Minas Gerais, Av. Antônio Carlos 6627, Pampulha, 31270-901 Belo Horizonte, MG, Brazil
c Departamento de Fisiologia e Biofísica, Instituto de Ciências Biológicas, Universidade Federal de Minas Gerais, Av. Antônio Carlos 6627, Pampulha, 31270-901 Belo Horizonte, MG, Brazil
*d Departamento de Química, Instituto de Ciências Exatas, Universidade Federal de Minas Gerais, Av. Antônio Carlos 6627, Pampulha, 31270-901 Belo Horizonte, MG, Brazil*
e Departamento de Física, Instituto de Ciências Exatas, Universidade Federal de Minas Gerais, Av. Antônio Carlos 6627, Pampulha, 31270-901 Belo Horizonte, MG, Brazil

References

1   J. Alvar, I.D. Vélez, C. Bem, M. Herrero, P. Desjeux, J. Cano, K. Jannin and M. de Boer, PLoS One, 2012, 7, e35671.
2   J.J. Shaw (Ed), World Class Parasites, Leishmania Kluwer Academic Publishers, Boston, Dordrecht, London, 2003.
3   D. Sereno, M. Cavaleyra, K. Zemzoumi, S. Maquaire, A. Ouaissi and J.L. Lemesre, Antimicrob. Agents Chemother., 1998, 42, 3097.
4   WHO-World Health Organization, Ethiopia, Addis Ababa, March, 22, 2007.
5   N. Shakya, A.S. Sane, P. Vishwakarma and P. Bajpai, Acta Trop., 2011, 119, 193.
6   L.H. Freitas-Junior, E. Chatelain, H.A. Kim and J.L. Siqueira-Neto, Int. J. Parasitol. Drugs Drug Resist., 2012, 2, 19.
7   F. Frézard, C. Demicheli, C.S. Ferreira and M.A.P. Costa, Antimicrob. Agents Chemother., 2001, 45, 913.
8   P. Shaked-Mishan, N. Ulrich, M. Ephros and D. Zilberstein, J. Biol. Chem., 2001, 276, 3971.
9   S. Wyllie, M.L. Cunningham and A.H. Fairlam, J. Biol. Chem., 2004, 279, 39925.
10   C. Demicheli and F. Frézard, Drug Des. Rev., 2005, 2, 243.
11   F. Frézard, D.A. Schettini, O.G.F. Rocha and C. Demicheli, Quim. Nova, 2005, 28, 511.
12   E.D. Franke, Ann. Intern. Med., 1990, 113, 934.
13   M. Goldberg, R. Langer and X. Jia, Biomater. Sci. Polym., 2007, 18, 241.
14   P.M. Mendes, Chem. Soc. Rev., 2013, 42, 9207.
15   S. Chander and D.W. Fuerstenau, Colloids Surf., 1982, 4, 101.
16   E.E. Connor, J. Mwamuka J, A. Gole, C.J. Murphy and M.D. Wyatt, Small, 2005, 1, 325.
17   Z.P. Xu, Q.H. Zeng, G.Q. Lu and A.B. Yu, Chem. Eng. Sci., 2006, 61, 1027.
18   A.H. Faraji and P. Wipf, Bioorg. Med. Chem., 2009, 17, 2950.
19   W. Gao, J.M. Chan and O.C. Farokhzad, Mol. Pharm., 2010, 7, 1913.
20   A. Tabakovic, M. Kester and J.H. Adair, WIREs Nanomed. Nanobiotechnol., 2012, 4, 96.
21   W. Paul and C.P. Sharma, Process Biochem., 2012, 47, 882.
22   S. Bisht, G. Bhakta, S. Mitra and A. Maitra, Int. J. Pharm., 2005, 288, 157.
23   S. Radin, J.T. Campbell, P. Ducheyne and J.M. Cuckler, Biomaterials, 1997, 18, 777.
24   S. Gordon, J. Todd, Z. A. Cohn, J Exp Med, 1974, 5, 1248.
25   T. Mosmann, J. Immunol. Methods, 1983, 65, 55.
26   Y. Liu, D.A. Peterson, H. Kimura and D. Schubert, J. Neurochem., 1997, 69, 593.
27   A. Dutta, S. Bandyopadhyay and C. Mandal, M. Parasitol. Int., 2005, 54, 119.
28   A.G. Tempone, D. Perez, S. Rath, A.L. Vilarinho, R.A. Mortara and H.F. Andrade, J. Antimicrob. Chemother., 2004, 54, 60.
29   W.L Roberts and P.M. Rainey, Anal. Biochem., 1993, 211, 1.
30   A. Gebre-Hiwot, G. Tadesse, S. L. Croft and D. Frommel, Acta Trop., 1992, 51, 245.
31   C. Bogdan, H. Moll, W. Solbach and M. Rollinghoff, Eur. J. Immunol., 1990, 20, 1135.
32   J. Kreuter, P. Ramge, V.E. Petrov, S. Hamm, S.E. Gelperina, B. Engelhardt, R.N. Alyautdin, H. von Briesen and D. Begley, J. Pharm. Res., 2003, 20, 409.
33   V. Sokolova, D. Koslova, T. Knuschke, J. Buer, A. Westendorf and M. Eplle, Acta Biomater., 2013, 9, 7527.
34   S. Sortino, A. Mazzaglia, L.M. Scolaro, F.M. Merlo, V. Valveri and M.T. Sciortino, Biomaterials, 2006, 27, 4256.
35   K. Ganesan, A. Kovtun, S. Neumann, R. Heuman and M. Eplle, J. Mater. Chem., 2008, 31, 3617.
36   J.D. Corrêa Júnior, M.I. Bruno, S. Allodi and M. Farina, J. Struct. Biol., 2008, 166, 59.
37   K. Simkiss, in Mechanisms and Phylogeny of Mineralization in Biological Systems, ed. S. Suga and H. Nakahara, Springer-Verlag, 1991, 382.
38   S. Soflaei, A. Dalimi, F. Ghaffarifar, M. Shakibaie, A.R. Shahverdi and M. Shafierpour, J. Parasitol. Res., 2012, doi:10.1155/2012/756568
39   S. Soflaei, A. Dalimi, A. Abdoli, M. Kamali, V. Nasiri and M. Shakibaie, Tat M. Comp. Clin. Pathol., DOI 10.1007/s00580-012-1561-z. 2012.
40   I. Ramírez-Macias, C.R. Maldonado, C. Marín, F. Olmo, R. Gutiérrez-Sánchez, M.J. Rosales, M. Quirós, J.M. Salas and M. Sánchez-Moreno, J. Inorg. Chem., 2012, 112, 1.
41   ATSDR – Agency for toxic substances and disease registry, Nickel, 2005.
42   A. Allahverdiyev, E.S. Abamor, M. Bagirova, S.Y. Baydar, S.C. Ates, F. Kaya, C. Kaya and M Rafailovich, Exp. Parasitol., 2013, 135.
43   S. Rath, W.F. Jardim and J.G. Dorea, Fresen. J. Anal. Chem., 1997, 4, 548.
44   E.M.D. Flores, E.P. dos Santos, J.S. Barin, R. Zanella, V.L. Dressler and C.F. Bittencourt, J. Anal. At. Spectrom., 2002, 17, 819.
45   L.A. Trivelin, J.R. Rohwedder and S. Rath, Talanta, 2006, 68, 1536.
46   V.G.K. Almeida, M.F. Lima and R.J. Cassella, Talanta, 2007, 71, 1047.
47   L.M. Cabral, V.N.M. Juliano, L.R.S. Dias, C.B. Dornelas, C.R. Rodrigues, M. Villardi, H.C. Castro and T.C. Santos, Mem. Inst. Oswaldo Cruz., 2008, 103, 130.
48   V.S. Santos, W.J.R. Santos, L.T. Kubota and C.R.T. Tarley, J. Pharm. Biomed. Anal., 2009, 50, 151.
49   L. Lukaszczyk and W. Zyrnicki, J. Pharm. Biomed. Anal., 2010, 52, 747.
50   F. Seby, C. Gleyzes, O. Gross, B. Plau and O.F.X. Donard, Anal. Bioanal. Chem., 2012, 404, 2939.
51   C. Hansen, E.W. Hansen, H.R. Hansen, B. Gammelgaard and S. Sturup, Trace Elem. Res., 2011, 144, 234.

52 W.L. Roberts, J.D. Berman and P.M. Rainey, Antimicrob. Agents Chemother., 1995, 39, 1234.

53 A.C. Cunningham, Exp. Mol. Pathol., 2001, 72, 132.

54 P. Mitropoulos, P. Konidas and M. Drukin-Konidas, J. Am. Acad. Dermatol., 2010, 63, 2.

55 C.R. Alving and G.M. Swartz, in Liposome Technology, ed. G. Gregoriadis, CRC Press, Boca Raton, 1984, vol. II, cap. 4.

56 A.K. Agrawal and C.M. Grupta., Adv. Drug Deliv. Rev., 1999, 41, 146.

57 V.P. Torchilin, Nat. Rev Drug Discov., 2005, 4, 160.

58 F.R. Fernandes, W.A. Ferreira, M.A. Campos, G.S. Ramos, K.C Kato, G.G. Almeida, J.D. Corrêa Júnior, M.N. Melo, C. Demicheli and F. Frezard, Antimicrob. Agents Chemother., 2013, 9, 57.

59 S.E.T. Borborema, R.A. Schwendener, J.A. Osso Jr. and H.F de Andrade Jr., Int. J. Antimicrob. Agents, 2011, 38, 347.

60 J. Esmaeili, M. Mohebali, G.H. Edrissian, S.M. Rezayat, M. Ghazi-Khansai and S. Charehdar, Acta Med. Iran., 2008, 43, 196.

61 A. Kornberg, in Horizons in Biochemistry, ed. M. Kasha and B. Pullman, Academic Press, New York, 1962, 264

62 T. Shintani, T. Uchiumi, T. Yonezawa, A. Salminen, A.A. Baykov, R. Lahti and A. Hachimori, FEBS Lett., 1998, 439, 263.

63 T.W. Young, N.J. Kuhn, A. Wadeson, S. Ward, D. Burges and G.D. Cooke, Microbiology, 1998, 144, 2563.

64 M.C. Merckel, I.P. Fabrichniy, A. Salminen, N. Kalkkinen, A.A. Baykov, R. Lahti and A. Goldman, Structure (Camb.), 2001, 9, 289.

65 S. Ahn, A.J. Milner, K. Futterer, M. Konopka, M. Ilias, T.W. Young and S.A. White., J. Mol. Biol., 2001, 313, 797.

66 D.L. Nelson and M.M. Cox, M.M. Lehninger Principles of Biochemistry, 3rd edn, Mc Millan, Worth Publishers, 2002.

67 N.N. Rao, M. Goméz-Garcia and A. Kornberg, Annu. Rev. Biochem, 2009, 78, 605.

68 S. Wyllie and A.H. Fairlamb, Biochem. Pharmacol., 2006, 71, 257.

69 L.G. Goodwin and J.E. Page, Biochem. J., 1943, 37, 198.

70 M. Das, S.B. Mukherjee and C. Shaha, J. Cell Sci., 2001, 114, 2461.

71 H. Zangger, J.C. Mottram and N. Fasel, Cell Death Differ., 2002, 9, 1126.

72 C.S. Ferreira, P.S. Martins, C. Demicheli, C. Brochu, M. Ouellette and F. Frézard, Biomaterials, 2001, 16, 441.

73 C. Shaha, Indian J. Med. Res., 2006, 123, 233.

74 S.A. Dzamitika, C.A. Falcão, F.B. de Oliveira, C. Marbeuf, A. Garnier-Suillerot, C. Demicheli, B. Rossi-Bergmann and F. Frézard, Chem. Biol. Interact., 2006, 160, 217.

75 T.P. Stossel, J. Cell Biol., 1973, 58, 346.

76 J.M. Alexiewicz, D. Kumar, M. Smogorzewski, M. Klin and S.G. Massry, Ann. Intern. Med., 1995, 123, 919.

77 S. Massry and M. Smogorzewski, Kidney Int. Suppl., 2001, 78, 195.

78 K. Tejle, K.E. Magnusson and B. Rasmusson, Biosci. Rep., 2002, 22, 529.

79 Z.A. Malik, C.R. Thompson, S. Hashimi, B. Porter, S.S Iyer and D.J. Kusner, J. Immunol., 2001, 170, 2811.

80 P. Nunes and N. Demaurex, J. Leukoc. Biol., 2010, 88, 22

81 M. Olivier, D.J. Gregory and G. Forget, Clin. Microbiol. Rev., 2005, 18, 293.

82 S. Scianimanico, M. Desrosiers, J.F. Dermine, S. Méresse, A. Descoteaux and M. Desjardins, Cell Microbiol., 199, 1, 19.

83 A. Holm, K. Tejle, K.E. Magnusson, A. Descoteaux and B. Rasmusson, Cell Microbiol., 2001, 3, 439.

84 A.F. Vinet, M. Fukuda, S.J. Turco and A. Descoteaux, PLoS Pathog., 2009, 5, doi: 10.1371/journal.ppat.1000628.
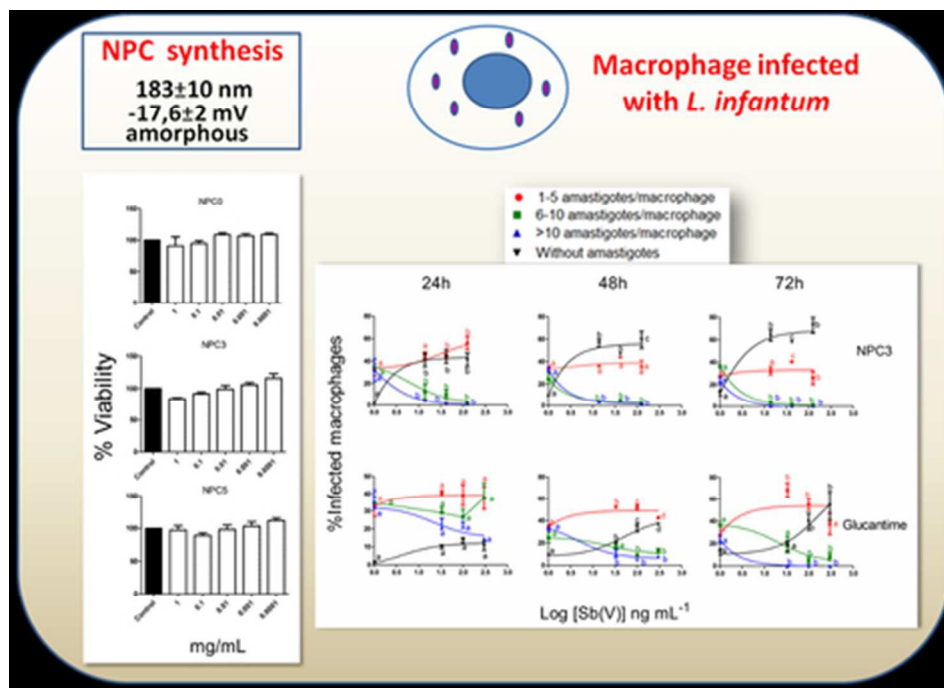
Nontoxic NPC containing Sb(V) boosts the infected macrophage recovery.
40x28mm (300 x 300 DPI)